PHYSICAL REVIEW D **80,** 125007 (2009)

Color magnetic flux tubes in dense QCD

Minoru Eto[1,*] and Muneto Nitta[2,†]

[1]*Theoretical Physics Laboratory, RIKEN, Saitama 351-0198, Japan*

[2]*Department of Physics, and Research and Education Center for Natural Sciences, Keio University, 4-1-1 Hiyoshi, Yokohama, Kanagawa 223-8521, Japan*

(Received 28 July 2009; published 4 December 2009)

QCD is expected to be in the color-flavor locking phase in high baryon density, which exhibits color superconductivity. The most fundamental topological objects in the color superconductor are non-Abelian vortices which are topologically stable color magnetic flux tubes. We present numerical solutions of the color magnetic flux tube for diverse choices of the coupling constants based on the Ginzburg-Landau Lagrangian. We also analytically study its asymptotic profiles and find that they are different from the case of usual superconductors. We propose the width of color magnetic fluxes and find that it is larger than naive expectation of the Compton wavelength of the massive gluon when the gluon mass is larger than the scalar mass.

DOI: 10.1103/PhysRevD.80.125007 PACS numbers: 12.38.−t, 11.27.+d, 25.75.Nq

I. INTRODUCTION

One of the important problems for understanding the strong interaction is to determine the phase diagram of QCD. In the very high density region with a large chemical potential at low temperature, it is expected that QCD is in the color-flavor locking (CFL) phase which exhibits color superconductivity [1,2]. There is the $SU(3)_{\mathrm{L}} \times SU(3)_{\mathrm{R}}$ flavor symmetry acting on light quarks u, d, and s when their masses are very small compared to the chemical potential. The $SU(3)_{\mathrm{C}}$ color symmetry is locked with the flavor symmetry by the condensations

$$\Phi_{\mathrm{R}} \sim \langle \psi_{\mathrm{R}} \sigma_2 \psi_{\mathrm{R}} \rangle, \qquad \Phi_{\mathrm{L}} \sim \langle \psi_{\mathrm{L}} \sigma_2 \psi_{\mathrm{L}} \rangle, \tag{1.1}$$

where $\psi_{\mathrm{L,R}}$ are the quark fields. Apart from the discrete symmetry the symmetry of the system is

$$G = SU(3)_{\mathrm{C}} \times SU(3)_{\mathrm{L}} \times SU(3)_{\mathrm{R}} \times U(1)_{\mathrm{B}}, \tag{1.2}$$

where the first element and the rests stand for gauge and flavor symmetries, respectively. We assume that the ground state is the positive parity state $\Phi_{\mathrm{R}} = \Phi_{\mathrm{L}} \equiv \Phi$ which would be determined by the instanton effect, so the chiral symmetry is broken to $SU(3)_{\mathrm{L+R}}$ which we write $SU(3)_{\mathrm{F}}$. The color superconductivity is expected to be realized in the core of a neutron star.

In the usual superconductors the gauge group $U(1)$ for the electromagnetic force is broken in the vacuum where electrons condensate to make a Cooper pair. When the superconductor is in the external magnetic fields which are above the critical value, magnetic fields inside the superconductor are squeezed and quantized. Consequently, there appear Abrikov-Nielsen-Olesen (ANO) vortices as magnetic flux tubes which topologically wind the spontaneously broken $U(1)$ [3,4]. The stability of the superconductor under the external magnetic fields is determined by static forces among vortices. If the force is repulsive (type II) the superconductor is stable; whereas if the force is attractive (type I) it is unstable. In the former the vortices constitute the so-called Abrikosov lattice [3]. Therefore understanding the interaction between vortices is very important to study stability of superconductors.

The types of color superconductor (type I or type II), which characterize a response to external magnetic fields, were studied in [5] by considering a domain wall separating the normal phase and the superconducting phase. They concluded that it is of type I in the weak coupling region. It is, however, more important to study vortices in the color superconductor, in order to understand its stability or a response to (external) *color* magnetic fields and/or rotation of the media which exhibits superfluidity too.[1] Color magnetic vortices were studied in [7–9] but these are unstable to decay because they are not topologically protected. On the other hand, the superfluid vortices which wind the broken $U(1)_{\mathrm{B}}$ appear in a response to rotation [8,10]. They are topologically stable but are dynamically unstable as we discuss below.

*meto@riken.jp

†nitta@phys-h.keio.ac.jp

[1]In a realistic situation such as a neutron star, the external color magnetic field cannot be considered because it is in the confining phase outside the core of a neutron star. Our statement about a response to color magnetic field is of a theoretical interest. The vortex here should be created under a rapid rotation of superfluids, or under a phase transition in a rapid cooling of a neutron star by the Kibble-Zurek mechanism [6].

The most fundamental objects are non-Abelian vortices carrying color magnetic fluxes [6,11,12], which were called the semisuperfluid vortices. Let us explain these objects. The order parameter space, parametrized by (would-be) Nambu-Goldstone (NG) modes of the symmetry breaking in the CFL phase, is

$$M \simeq \frac{SU(3) \times U(1)}{\mathbb{Z}_3} = U(3). \tag{1.3}$$

These NG modes are eaten by the $SU(3)$ gauge fields (gluons) except for the $U(1)$ part. This has a nontrivial first homotopy group:

$$\pi_1(M) = \pi_1[U(3)] = \mathbb{Z}. \tag{1.4}$$

The $U(1)_{\rm B}$ vortex found in [8,10] is of the form $\Phi = vf(r)\mathbf{1}_3$ with the boundary conditions $f(r \to \infty) = 1$ and $f(r = 0) = 0$. However, this does not have a minimum winding number but has the triple of the minimum element. The fundamental vortex string with the minimum number is a non-Abelian vortex [6,11,12], for instance given as

$$\begin{aligned} &\Phi = v\,\mathrm{diag}(f(r)e^{i\theta}, g(r), g(r)), \\ &A_i \sim \frac{\epsilon_{ij}x^j}{r^2}[1 - h(r)]\,\mathrm{diag}(2, -1, -1) \end{aligned} \tag{1.5}$$

with the boundary conditions $f(r \to \infty)$, $g(r \to \infty) = 1$, $h(r \to \infty) = 0$ and $f(r = 0) = 0$, $g'(r = 0) = 0$, $h(r = 0) = 1$. The asymptotic behavior ($r \to \infty$) of the scalar field of the non-Abelian vortex is

$$\begin{aligned} \Phi &\to v\,\mathrm{diag}(e^{i\theta}, 1, 1) \\ &= ve^{i(\theta/3)}\mathrm{diag}(e^{i(2\theta/3)}, e^{-i(\theta/3)}, e^{-i(\theta/3)}) \sim ve^{i(\theta/3)}\mathbf{1}_3, \end{aligned} \tag{1.6}$$

where the last denotes a gauge transformation by $U(r, \theta) = \mathrm{diag}(e^{-i(2/3)\theta E(r)}, e^{i(\theta/3)E(r)}, e^{i(\theta/3)E(r)})$ with an arbitrary function $E(r)$ satisfying the boundary conditions $E(r = 0) = 0$ and $E(r \to \infty) = 1$.[2] From Eq. (1.6) one can understand that the non-Abelian vortex has the $U(1)_{\rm B}$ winding $1/3$ of that of the $U(1)_{\rm B}$ superfluid vortex. The $U(1)_{\rm B}$ symmetry is global and so the tension (the energy per unit length) of a vortex string is logarithmically divergent in infinite space. Since the tension is proportional to the square of the winding number, the non-Abelian vortex has the tension $1/9$ of the one of the $U(1)_{\rm B}$ superfluid vortex. One $U(1)_{\rm B}$ superfluid vortex has the triple amount of the sum of the energies of three well-separated non-Abelian semisuperfluid vortices. Therefore the decay of the $U(1)_{\rm B}$ superfluid vortex into three non-Abelian semisuperfluid vortices is inevitable from the point of view of the energetics.

The non-Abelian semisuperfluid vortex (1.5) carries a color magnetic flux.[3] Color magnetic fluxes also exist in quark gluon plasma [14] but they are unstable.[4] Contrary to those, color magnetic flux tube (1.5) is topologically (and dynamically) stable. The vortex solution (1.5) breaks the color-flavor locked symmetry $SU(3)_{\rm C+F}$ down to its subgroup $[SU(2) \times U(1)]_{\rm C+F}$. Consequently, there appear further NG zero modes [11]:

$$\mathbb{C}P^2 = \frac{SU(3)_{\rm C+F}}{[SU(2) \times U(1)]_{\rm C+F}}. \tag{1.7}$$

This space parametrizes a continuous family of the vortex solutions. These zero modes are called orientational zero modes.[5] All solutions of the continuous family in Eq. (1.7) have the same tension and the same boundary condition (1.6) up to a regular gauge transformation. Therefore the orientational zero modes of $\mathbb{C}P^2$ (1.7) are normalizable and can be regarded as the genuine moduli (collective coordinates) of the vortex [18]. It corresponds one to one to the color magnetic flux which the vortex carries.

As in usual superconductors, the (in)stability of the color superconductor in the presence of the (external) color flux is determined by the interaction between non-Abelian semisuperfluid vortices (color magnetic fluxes) given in Eq. (1.5). The asymptotic interaction between two well-separated non-Abelian semisuperfluid vortices has been calculated [11,12] in which the universal repulsion has been found. This calculation is valid when the distance between them is much larger than the Compton wavelengths of massive particles, which are essentially the penetration depth and the coherence length. In this region, semisuperfluid vortices are essentially $U(1)_{\rm B}$ global vortices with the winding number $1/3$ as in Eq. (1.6) and, in fact, the static force between them is $1/3$ of that between two $U(1)_{\rm B}$ vortices [11,12]. This result implies important consequences. First, the color superconductor is stable in the presence of the (external) color magnetic fields. Non-Abelian semisuperfluid vortices will constitute a lattice, at

[2]This transformation is well defined in the whole space because of the triviality of the first homotopy group: $\pi_1[SU(N)] = 0$.

[3]The authors in [13] studied different kinds of magnetic flux tubes in dense QCD. Although the authors called them "gluon vortices," those are magnetic for the usual electromagnetic (EM) force of $U(1)_{\rm EM}$ [mixed with one color component of $SU(3)_{\rm C}$]. The important difference between their flux tubes and our color magnetic flux tubes is that their vortices are generated by the unbroken generator and therefore topologically trivial, while our vortices are generated by the broken generators and consequently topologically nontrivial. We will give some comments in the discussion.

[4]Those flux tubes are topological unstable but it was discussed in [15] that they are dynamically metastable.

[5]The idea was brought from non-Abelian vortices in supersymmetric $U(N)$ gauge theories. In this case the overall phase $U(1)_{\rm B}$ is also gauged and the vortices are local vortices with finite tension [16], unlike non-Abelian semisuperfluid vortices. See [17] for a review.

least when the lattice spacing is much larger than the penetration depth and the coherence length. Second, the $U(1)_{\rm B}$ superfluid vortex is unstable to decay into three non-Abelian semisuperfluid vortices because of the repulsion among them, at least for large fluctuations. Each semisuperfluid vortex carries different color magnetic flux with the total color being canceled out. In the core of neutron star, one can expect that the $U(1)_{\rm B}$ superfluid vortices are first created in a response to rotation of the star. Then each of them must be broken into three semisuperfluid vortices which will constitute the lattice of color magnetic flux tubes. The phase boundary of the CFL and hadronic phase was studied in [19] in an application to the neutron star physics.

However, the interaction obtained in [11,12] is not valid when two vortices are closer such that the distance between them is of the order of the Compton wavelengths. We need to know the core structure of the vortex in order to study short range interactions. In the analysis of Balachandran *et al.* [6], they used an approximation for profile functions in (1.5): they assumed a constant g and solved the equation for f only. This is not a good approximation around the core of the vortex. In fact, as we show in this paper, the profile of g significantly differs from the constant for some parameter region.

In this paper we study the profile functions of non-Abelian semisuperfluid vortices in detail as a first step to study the short range interaction of them. First, we study the asymptotic tails of the profile functions by analytically studying the equations of motion, and find that they are different from the case of the ANO vortex in usual superconductors where the tails of the $U(1)$ gauge field with mass m_e and the scalar field with mass m_H decay exponentially as e^{-m_e} and e^{-m_H}, respectively; on the other hand, the both tails of the scalar and gauge fields of a non-Abelian superfluid vortex behave as e^{-m} with the lighter mass m among the masses m_G for massive gluons and m_χ for massive traceless scalar fields. We then construct numerical solutions for diverse choices of the coupling constants, by using the relaxation method with the appropriate boundary conditions. By the numerical solutions we determine the coefficients in the asymptotic solutions. We propose the width of the color magnetic flux by the diffractiveness weighted by the magnetic flux. We calculate it numerically and confirm the above estimation of the tails. Therefore we conclude that the width of the color magnetic flux is significantly different from the naive expectation of the Compton wavelength (the penetration depth) of the massive gluons when the gluon mass m_G is larger than the mass m_χ of the traceless scalar fields; in general, the width approaches to a constant depending of m_χ not behaving as m_G^{-1}.

Throughout this paper we turn off the electromagnetic interaction $U(1)_{\rm EM}$ in order to study purely non-Abelian aspects of vortices. The inclusion of it does not change the properties found in this paper. However, the electromagnetic interaction explicitly breaks the flavor symmetry $SU(3)_{\rm F}$, since $U(1)_{\rm EM}$ is embedded into $SU(3)_{\rm F}$. Consequently, the orientation modes of $\mathbb{C}P^2$ get masses. This aspect remains as a future problem.

This paper is organized as follows. In Sec. II the Ginzburg-Landau Lagrangian is studied. We explain the symmetry structure in detail especially paying attention to the discrete symmetries. We also give the mass spectra of the CFL vacuum. In Sec. III we study the equations of motion in the cylindrical coordinates in the presence of a vortex. In Sec. IV asymptotic behaviors of the profile functions are studied analytically. In Sec. V we give numerical solutions of the profile functions and determine the coefficients of the asymptotic profile functions. We numerically evaluate the width of the color magnetic flux and compare it with the Compton wavelength of the massive gluons. Section VI is devoted to conclusion and discussions. We discuss the force between two semisuperfluid vortices at the short distance. We discuss that the intervortex force mediated by the exchange of the massive particles becomes comparable with the intervortex force mediated by the exchange of the massless $U(1)_{\rm B}$ NG boson. In the Appendix we discuss the general ansatz of the vortex in the diagonal entries.

II. THE NON-ABELIAN LANDAU-GINZBURG MODEL

Our starting point is the Ginzburg-Landau Lagrangian [7,20,21][6]

$$\mathcal{L} = \mathrm{Tr}\Big[-\frac{1}{4}F_{ij}F^{ij} + \nabla_i\Phi^\dagger\nabla^i\Phi - \lambda_2(\Phi^\dagger\Phi)^2 + \mu^2\Phi^\dagger\Phi\Big] - \lambda_1(\mathrm{Tr}[\Phi^\dagger\Phi])^2 - \frac{3\mu^4}{4(3\lambda_1+\lambda_2)}, \tag{2.1}$$

where the last constant term is introduced for the vacuum energy to vanish. Our notation is $\nabla_i = \partial_i - ig_sA_i$, $F_{ij} = \partial_iA_j - \partial_jA_i - ig_s[A_i, A_j]$, and $\mathrm{Tr}[T^aT^b] = \delta^{ab}$ for $a = 1, 2, \ldots, 8$. g_s is the $SU(3)_{\rm C}$ gauge coupling constant. For the stability of vacua, we consider the parameter region $\mu^2 > 0$, $\lambda_2 > 0$, and $3\lambda_1 + \lambda_2 > 0$. The action of color, flavor, and baryon symmetries on Φ is given by

$$\Phi \to e^{i\theta}U_{\rm C}\Phi U_{\rm F}, \qquad U_{\rm C} \in SU(3)_{\rm C}, \qquad U_{\rm F} \in SU(3)_{\rm F}, \qquad e^{i\theta} \in U(1)_{\rm B}. \tag{2.2}$$

There is some redundancy of the action of these symmetries. The actual symmetry is given by

$$G \equiv \frac{SU(3)_{\rm C}\times SU(3)_{\rm F}\times U(1)_{\rm B}}{(\mathbb{Z}_3)_{\rm C+B}\times(\mathbb{Z}_3)_{\rm F+B}}, \tag{2.3}$$

[6]The stiffness parameter in front of the kinetic term of Φ is set to be 1 by a field redefinition.

where the discrete groups in the denominator defined as follows do not change Φ and are removed from G;

$$(\mathbb{Z}_3)_{\mathrm{C+B}}: (w^k\mathbf{1}_3, \mathbf{1}_3, w^{-k}) \in SU(3)_{\mathrm{C}} \times SU(3)_{\mathrm{F}} \times U(1)_{\mathrm{B}}, \tag{2.4}$$

$$(\mathbb{Z}_3)_{\mathrm{F+B}}: (\mathbf{1}_3, w^k\mathbf{1}_3, w^{-k}) \in SU(3)_{\mathrm{C}} \times SU(3)_{\mathrm{F}} \times U(1)_{\mathrm{B}}, \tag{2.5}$$

$$w = e^{2\pi i/3}, \qquad k = 0, 1, 2. \tag{2.6}$$

For later use let us redefine the discrete symmetry in the denominator as $(\mathbb{Z}_3)_{\mathrm{C+B}} \times (\mathbb{Z}_3)_{\mathrm{F+B}} \simeq (\mathbb{Z}_3)_{\mathrm{C+F}} \times (\mathbb{Z}_3)_{\mathrm{C-F+B}}$ with

$$(\mathbb{Z}_3)_{\mathrm{C+F}}: (w^k\mathbf{1}_N, w^{-k}\mathbf{1}_N, 1) \in SU(3)_{\mathrm{C}} \times SU(3)_{\mathrm{F}} \times U(1)_{\mathrm{B}}, \tag{2.7}$$

$$(\mathbb{Z}_3)_{\mathrm{C-F+B}}: (w^k\mathbf{1}_N, w^k\mathbf{1}_N, w^{-2k}) \in SU(3)_{\mathrm{C}} \times SU(3)_{\mathrm{F}} \times U(1)_{\mathrm{B}}. \tag{2.8}$$

Next we discuss symmetry breaking in the vacua. By using the symmetry G, one can choose a vacuum expectation value as

$$\langle\Phi\rangle = v\mathbf{1}_3, \qquad v^2 \equiv \frac{\mu^2}{2(3\lambda_1 + \lambda_2)} > 0 \tag{2.9}$$

without loss of generality. By this condensation the gauge symmetry $SU(3)_{\mathrm{C}}$ is completely broken, and the full symmetry G is spontaneously broken down to

$$H = \frac{SU(3)_{\mathrm{C+F}} \times (\mathbb{Z}_3)_{\mathrm{C-F+B}}}{(\mathbb{Z}_3)_{\mathrm{C+B}} \times (\mathbb{Z}_3)_{\mathrm{F+B}}} = \frac{SU(3)_{\mathrm{C+F}}}{(\mathbb{Z}_3)_{\mathrm{C+F}}} \tag{2.10}$$

with

$$SU(3)_{\mathrm{C+F}}: (U, U^\dagger, 1) \in SU(3)_{\mathrm{C}} \times SU(3)_{\mathrm{F}} \times U(1)_{\mathrm{B}}. \tag{2.11}$$

Therefore as denoted in Eq. (1.3) the order parameter space (the vacuum manifold) is given by

$$M = G/H = \frac{SU(3)_{\mathrm{C-F}} \times U(1)_{\mathrm{B}}}{(\mathbb{Z}_3)_{\mathrm{C-F+B}}} \simeq U(3) \tag{2.12}$$

with

$$SU(3)_{\mathrm{C-F}}: (U, U, 1) \in SU(3)_{\mathrm{C}} \times SU(3)_{\mathrm{F}} \times U(1)_{\mathrm{B}}. \tag{2.13}$$

This space is parametrized by $SU(3)$ would-be NG bosons, which are eaten by $SU(3)_{\mathrm{C}}$ gauge bosons (gluons), and one massless NG boson of the spontaneously broken $U(1)_{\mathrm{B}}$.

The mass spectra around the Higgs vacuum (2.9) can be found by perturbing Φ as

$$\Phi = v\mathbf{1}_3 + \frac{\phi + i\varphi}{\sqrt{2}}\mathbf{1}_3 + \frac{\chi^a + i\zeta^a}{\sqrt{2}}T^a. \tag{2.14}$$

The trace parts ϕ and φ belong to the singlet of the color-flavor locked symmetry whereas the traceless part χ and ζ^a belong to the adjoint representation of it. The $SU(3)$ gauge fields (gluons) get mass with eating ζ^a by the Higgs mechanism. The masses of fields are given by

$$m_G^2 = 2g_s^2v^2, \qquad m_\phi^2 = 2\mu^2, \qquad m_\varphi^2 = 0, \qquad m_\chi^2 = 4\lambda_2 v^2, \tag{2.15}$$

where m_G is the mass of the $SU(3)$ massive gauge bosons (gluons) and φ is the NG boson associated with the spontaneously broken $U(1)_{\mathrm{B}}$ symmetry. The trace part ϕ and the traceless part χ of Φ are massive bosons. At the weak coupling regime [8] these masses are shown to be

$$m_G \gg m_\phi = 2m_\chi. \tag{2.16}$$

We would like to stress that this system has four different mass scales. As in usual superconductors, m_G^{-1} is the penetration depth and m_χ^{-1} is the coherence length. On the other hand, the massive boson ϕ with mass m_ϕ and the massless NG mode φ for the spontaneously broken $U(1)_{\mathrm{B}}$ are typical for the superfluid system with a superfluid vortex of the size m_ϕ^{-1}. Therefore the system is mixed up with the (non-Abelian) superconductor and the superfluid. This is why the authors of [6] called this system the semisuperfluid.

The interactions between two semisuperfluid vortices at large distance $r \gg \max\{m_\chi^{-1}, m_\phi^{-1}, m_G^{-1}\}$ are interpolated by the $U(1)_{\mathrm{B}}$ NG mode. As a result they repel each other by the long range force [11].

Once the vortices are placed at the distance of the scale $\mathcal{O}(m_{\chi,\phi,G}^{-1})$, we cannot ignore exchange of the massive particles, and the interaction must depend on mass ratios

$$\gamma_1 \equiv \frac{m_G}{m_\chi}, \qquad \gamma_2 \equiv \frac{m_\chi}{m_\phi}. \tag{2.17}$$

Therefore, the type of relatively short range interactions would not be so simple, unlike the type I/II classification for usual superconductors. For instance, there is no critical coupling limit where the interactions are completely canceled out in the case of the color superconductor. The actual interactions at intermediate distance may be quite complicated. See Secs. IV and VI for further discussion.

For later convenience, let us rewrite the Landau-Ginzburg potential in terms of the dimensionful parameters $\mu^2 = m_\phi^2/2$, $\lambda_1 = (m_\phi^2 - m_\chi^2)/(12v^2)$, and $\lambda_2 = m_\chi^2/(4v^2)$:

$$V = \frac{m_\phi^2}{12v^2}(\mathrm{Tr}[\Phi^\dagger\Phi - v^2\mathbf{1}_3])^2 + \frac{m_\chi^2}{4v^2}\,\mathrm{Tr}[\langle\Phi^\dagger\Phi\rangle^2], \tag{2.18}$$

where $\langle A\rangle$ stands for the traceless part of an N by N matrix A: $\langle A\rangle \equiv A - (1/N)\,\mathrm{Tr}A$.

III. EQUATIONS OF MOTION FOR A VORTEX

We would like to consider topologically stable vortex configurations supported by the first homotopy group in Eq. (1.4). Here we are interested in the minimally wound vortex solution. We make a diagonal ansatz for the minimally winding vortex in the cylindrical coordinates (r, θ, x_3),

$$\Phi(r,\theta) = \begin{pmatrix} e^{i\theta}f(r) & 0 & 0 \\ 0 & g(r) & 0 \\ 0 & 0 & g(r) \end{pmatrix},$$
$$A_i(r,\theta) = \frac{1}{g_s}\frac{\epsilon_{ij}x^j}{r^2}[1-h(r)]\begin{pmatrix} -2/3 & 0 & 0 \\ 0 & 1/3 & 0 \\ 0 & 0 & 1/3 \end{pmatrix}. \tag{3.1}$$

All other solutions are generated by the color-flavor symmetry. For later convenience let us rewrite the solutions (3.1) as

$$\Phi(r,\theta) = e^{i\theta((1/\sqrt{3})T_0 - \sqrt{(2/3)}T_8)}\left(\frac{F(r)}{\sqrt{3}}T_0 - \sqrt{\frac{2}{3}}G(r)T_8\right) \tag{3.2}$$

$$A_i(r,\theta) = \frac{1}{g_s}\frac{\epsilon_{ij}x^j}{r^2}[1-h(r)]\sqrt{\frac{2}{3}}T_8 \tag{3.3}$$

with the $U(3)$ generators

$$T_0 = \frac{1}{\sqrt{3}}\mathrm{diag}(1,1,1), \qquad T_8 = \frac{1}{\sqrt{6}}\mathrm{diag}(-2,1,1) \tag{3.4}$$

and the redefined profile functions

$$F \equiv f + 2g, \qquad G \equiv f - g. \tag{3.5}$$

Note that the first term proportional to T_0 in Φ in Eq. (3.2) is invariant under the color-flavor locking symmetry H in Eq. (2.10) while the second term proportional to T_8 (traceless part) breaks H down to $U(2)$. This symmetry breaking by T_8 gives rise to the NG zero modes $SU(3)/U(2) \simeq \mathbb{C}P^2$ associated with the vortices as in Eq. (1.7) [11]. Therefore the nonzero profile function $G(r)$ plays the role of the order parameter for this breaking of the color-flavor symmetry. With the ansatz (3.3), the color magnetic flux is given by

$$F_{12} = \frac{\sqrt{6}h'}{3g_s r}T_8. \tag{3.6}$$

Equations of motion for the profile function $f(r)$, $g(r)$, $h(r)$ are of the form

$$f'' + \frac{f'}{r} - \frac{(2h+1)^2}{9r^2}f - \frac{m_\phi^2}{6}f(f^2+2g^2-3) - \frac{m_\chi^2}{3}f(f^2-g^2) = 0, \tag{3.7}$$

$$g'' + \frac{g'}{r} - \frac{(h-1)^2}{9r^2}g - \frac{m_\phi^2}{6}g(f^2+2g^2-3) + \frac{m_\chi^2}{6}g(f^2-g^2) = 0, \tag{3.8}$$

$$h'' - \frac{h'}{r} - \frac{m_G^2}{3}(g^2(h-1) + f^2(2h+1)) = 0. \tag{3.9}$$

We solve these differential equations with the following boundary conditions:

$$\begin{aligned} &(f,g,h) \to (1,1,0) \quad \text{as } r \to \infty, \\ &(f,g',h) \to (0,0,1) \quad \text{as } r \to 0. \end{aligned} \tag{3.10}$$

The third terms in the left-hand side of Eqs. (3.7) and (3.8) are typical for global vortex configurations which leads logarithmic divergence of the tension.

The tension of the vortex string is given by

$$T = 2\pi v^2 \int dr r\left[f'^2 + \frac{(2h+1)^2}{9r^2}f^2 + 2\left(g'^2 + \frac{(h-1)^2}{9r^2}g^2\right) + \frac{h'^2}{3m_G^2 r^2} + \mathcal{V}\right], \tag{3.11}$$

$$\mathcal{V} = \frac{1}{12}v^2[(f^2+2g^2-3)^2 m_\phi^2 + 2(f^2-g^2)^2 m_\chi^2]. \tag{3.12}$$

This diverges as $T \sim \frac{2\pi v^2}{3}\log L/r_0$ with L being an IR cutoff scale, the size of the system, and r_0 being a typical scale $r_0 \sim m_\phi^{-1}$. The factor $1/3$ reflects the fact that the minimum winding vortex winds $1/3$ of $U(1)_{\mathrm{B}}$.

We will see that the color magnetic flux in Eq. (3.6) is well squeezed and becomes a well localized tube even though the energy of the vortex itself logarithmically diverges.

Here let us make comments on related vortices in the CFL phase. Another color magnetic vortex in the CFL phase studied in [9] is generated by only T_8 [mixed with electromagnetic $U(1)_{\mathrm{EM}}$] without the part of T_0 in Eq. (3.2). For the single valuedness of fields the minimum winding is the triple of our color magnetic flux, and consequently it carries the triple amount of ours. It is, however, unstable because $\pi_1[SU(3)_C]$ is trivial. On the other hand, the global $U(1)_{\mathrm{B}}$ vortex which is made by only the generator of global symmetry T_0 has been studied in [8,10]. It carries neither a color magnetic flux nor internal orientations. Since such a configuration cannot be combined with $SU(3)$, it is necessary to wind 2π along T_0, and consequently it has the triple winding of our color magnetic flux. As stated in the Introduction, it decays into three semi-superfluid vortices which have different color fluxes with the total flux canceled out.

Before closing this section, let us give a comment on a relation to a non-Abelian global vortex which appears

when the chiral symmetry is spontaneously broken in the $U(N)$ linear sigma model [22–25]. The linear sigma model is realized from our Lagrangian by just ungauging $SU(N)_C$, namely, turning off the gauge coupling $g_s = 0 (m_G = 0)$. At the level of equations of motion, it is enough to set $h(r) = 1$. Then Eq. (3.9) becomes trivial and we are left with Eqs. (3.7) and (3.8) (with $h = 1$) which are nothing but equations of motion for the non-Abelian global vortices [23,25]. However, $h(r) = 1$ is inconsistent with the boundary condition (3.10), and so the non-Abelian global vortices cannot be obtained in a continuous limit of the non-Abelian semisuperfluid vortex.

IV. ASYMPTOTICS

Let us next study the asymptotics in the region $r \gg \max\{m_\chi^{-1}, m_\phi^{-1}, m_G^{-1}\}$. The configuration is almost vacuum in such a region, so it is useful for us to use the profile function F, G rather than f, g in Eqs. (3.7) and (3.8). Let us perturb the fields by

$$F = 3 + \delta F, \qquad G = \delta G, \qquad h = \delta h, \qquad (|\delta F|, |\delta G|, |\delta h|) \ll 1, \tag{4.1}$$

and linearize the equations of motion as

$$\left(\triangle - m_\phi^2 - \frac{1}{9r^2}\right)\delta F = \frac{1}{3r^2}, \tag{4.2}$$

$$\left(\triangle - m_\chi^2 - \frac{1}{9r^2}\right)\delta G = \frac{2}{3r^2}\,\delta h, \tag{4.3}$$

$$\delta h'' - \frac{\delta h'}{r} - m_G^2 \delta h = \frac{2}{3} m_G^2 \delta G, \tag{4.4}$$

where $\triangle \equiv \frac{1}{r}\partial_r(r\partial_r)$.[7] The last equation can be rewritten with $\delta\tilde{h} = \delta h/(m_G r)$ as

$$\left(\triangle - m_G^2 - \frac{1}{r^2}\right)\delta\tilde{h} = \frac{2}{3} m_G \frac{\delta G}{r}. \tag{4.5}$$

The equations for δF are the same with the one for a global $U(1)$ vortex with the winding number $1/3$.

First let us solve Eq. (4.2). The equation with the right-hand side being zero, $[\triangle - m_\phi^2 - 1/(9r^2)]\delta F = 0$, has a solution $q_\phi K_{1/3}(m_\phi r)$ with q_ϕ being an integration constant. Here $K_{1/3}(r)$ is one of the modified Bessel functions $K_n(r)$ of the 2nd class, which solves

$$\left(\triangle - m^2 - \frac{n^2}{r^2}\right)K_n(mr) = 0. \tag{4.6}$$

It is known that $K_n(r)$ with $0 \le n \le 1$ is well approximated by $K_{1/2}(r) = \sqrt{\frac{\pi}{2r}}e^{-r}$ at $r \gg 1$. So we get

$$\delta F = q_\phi \sqrt{\frac{\pi}{2m_\phi r}} e^{-m_\phi r} + \left(-\frac{1}{3m_\phi^2 r^2} + \mathcal{O}\left(\frac{1}{(m_\phi r)^4}\right)\right). \tag{4.7}$$

Since $K_n(r)$ is much smaller than $1/r^2$ for $r \gg 1$, the first term can be neglected as in the case of the $U(1)$ global (superfluid) vortex. We will not discuss the coefficient q_ϕ below.

Let us next solve Eqs. (4.3) and (4.5). Clearly, the solution cannot have a tail decreasing with a polynomial. They have exponentially small tails similarly to the ANO vortex in the superconductor. The equations with the right-hand sides of Eqs. (4.3) and (4.5) being zero can be solved by

$$\delta G \simeq q_\chi K_{1/3}(m_\chi r) \simeq q_\chi \sqrt{\frac{\pi}{2m_\chi r}} e^{-m_\chi r}, \qquad \delta h \simeq q_G m_G r K_1(m_G r) \simeq q_G \sqrt{\frac{\pi m_G r}{2}} e^{-m_G r}, \tag{4.8}$$

where q_χ and q_G are integration constants, which are determined numerically in the next section. Let us take into account the corrections from the right-hand sides of Eqs. (4.3) and (4.5). When the inequality $m_G \gtrapprox m_\chi$ holds, we can ignore $\delta h \sim e^{-m_G r}$ in Eq. (4.3). So $\delta G \sim e^{-m_\chi r}$ in Eq. (4.8) is a good approximation. However, we cannot discard δG in Eq. (4.4) since $\delta G \simeq e^{-m_\chi r} \gg e^{-m_G r}$. We thus find the following approximations:

$$\delta G = q_\chi \sqrt{\frac{\pi}{2m_\chi r}} e^{-m_\chi r}, \qquad \delta h = -\frac{2q_\chi}{3}\frac{m_G^2}{m_G^2 - m_\chi^2}\sqrt{\frac{\pi}{2m_\chi r}} e^{-m_\chi r} \quad \text{for } m_G \gtrapprox m_\chi (\gamma_1 \gtrapprox 1). \tag{4.9}$$

On the other hand, when the other inequality $m_\chi \gtrapprox m_G$ holds, we should reconsider approximation for δG. In the same way we find the approximations

$$\delta G \simeq -\frac{2q_G}{3}\frac{1}{(m_\chi^2 - m_G^2)r^2}\sqrt{\frac{\pi m_G r}{2}} e^{-m_G r}, \qquad \delta h \simeq q_G \sqrt{\frac{\pi m_G r}{2}} e^{-m_G r} \quad \text{for } m_\chi \gtrapprox m_G (\gamma_1 \lessapprox 1). \tag{4.10}$$

These are not good approximations for $m_\chi \approx m_G$. For the regions $m_\chi \not\gtrless m_G$, we find from Eqs. (4.9) and (4.10) that both the massive traceless scalars χ and the massive gauge

[7] If we consider the local vortex by gauging $U(1)_B$, all the linearized equations at the asymptotic region become the form of $(\triangle - m_X^2)\delta X = 0$ [26]. Here symbol X stands for all the fields, namely Abelian, non-Abelian gauge fields, and all the scalar fields.

fields (gluons) have the same asymptotic behavior with the exponential tails e^{-mr} with the common mass $m \equiv \min\{m_\chi, m_G\}$. These asymptotic behaviors are quite different from the ANO vortex in usual superconductors.[8]

Now we can roughly estimate the width of the color magnetic flux tube given in Eq. (3.6). It can be read from the tail δh of the gauge fields. Namely, it can be estimated by the Compton wavelengths m^{-1} with $m = \min\{m_\chi, m_G\}$. It is the Compton wavelength of massive gluons (penetration depth) as expected when $m_\chi > m_G (\gamma_1 < 1)$, while it is no longer the case when $m_G > m_\chi (\gamma_1 > 1)$: contrary to the naive expectation the tail of gauge field decays at the Compton wavelength of massive traceless scalar field χ (coherence length).[9] In Sec. V these estimations are confirmed by the numerical calculations.

The $U(1)_{\rm B}$ NG boson makes the powerlike tails in the traceless part of Φ which is color-flavor singlet as seen in Eq. (4.7). So the powerlike tail is dominated at the large distance from the core of the non-Abelian semisuperfluid vortex. It yields the logarithmic divergence in the tension of the vortex and leads to the long range repulsive forces between two vortices [11]. As we approach the vortex core from the large distance, we see the exponential tails behaving as $e^{-m_\phi r}$, $e^{-m_\chi r}$, $e^{-m_G r}$. We will first come across the tail of the fields with the lightest mass.

When m_ϕ is the lightest mass, the semisuperfluid vortex behaves as the usual superfluid vortex [with $1/3$ $U(1)_{\rm B}$ winding], since the massive singlet scalar field ϕ exists also in a usual $U(1)$ superfluid vortex. In general, the exchange of the massive scalar field leads to an attractive interaction (as in usual superconductors), and so we expect that the short range interaction is attractive. In this case non-Abelian properties are somewhat hidden inside the core of the superfluid vortex.

More interesting is the case that m_χ (or m_G) is the smallest, since the asymptotic tail which we first come across is those in Eq. (4.9) [or Eq. (4.10)]. There are two remarkable points. (i) The asymptotic behaviors are quite different from the ANO vortex in usual superconductors. The interactions of ANO vortices depend on the ratio of the masses of the massive gauge boson and the massive scalar field, giving classification of type I and II as denoted in footnote [8]. In Eqs. (4.9) and (4.10) we find that both the scalar and vector fields have the asymptotic tails of the same order e^{-mr} with $m = \min\{m_\chi, m_G\}$, as already pointed out. So we may have to consider two contributions equivalently. (ii) The interactions may depend on the internal orientation moduli $\mathbb{C}P^2$. In fact, in the case of the local $U(N)$ vortices for which $U(1)_{\rm B}$ is gauged, the exchanging of the particles which are not singlet but in the adjoint representation of the color-flavor symmetry leads to interactions depending on the internal orientations [28]. In order to get better understanding about the short range interactions between non-Abelian semisuperfluid vortices, we need more qualitative and quantitative studies which is beyond the scope of this paper. However, see further discussion in Sec. VI.

V. NUMERICS: SOLUTIONS AND WIDTH OF COLOR MAGNETIC FLUX

In this section we provide numerical solutions. We use the relaxation method with appropriate boundary conditions, see Fig. 1. We see that the interiors of the vortices depend on the ratios γ_1 and γ_2.

Some numerical solutions were previously found in [6] with the approximation of $g(r) = 1$ in Eq. (3.2). Although this approximation makes numerical calculation easier, the authors of [6] did not evaluate the validity of the approximation. Note that $g(r) = 1$ is never true unlike the case of non-Abelian global vortex [25] and the non-Abelian local vortex [26], in whose cases the unwinding fields can be constant for particular values of coupling constants. Moreover, $G = f - g$ plays the role of the order parameter for the breaking of the $SU(3)_{\rm C+F}$, so we need the profile function $g(r)$. As we can see from the boundary condition (3.10), $g(0)$ is not fixed and this is a typical parameter to characterize the solutions. We find $0 \le g(0) \le \sqrt{3/2}$ where $g(0) \to 0$ as $m_\chi \to \infty$ and $g(0) \to \sqrt{3/2}$ as $m_\phi \to \infty$. This can be understood by considering $m_\chi \to \infty$ in Eq. (2.18) which forces $f^2 + 2g^2 = 3$ while $m_\phi \to \infty$ imposes $f = g$. Qualitatively speaking, we find $g(0) < 1$ when $m_\phi < m_G$, and $1 < g(0)$ for $m_\chi < m_\phi$. In the case of $m_\phi = m_\chi$, the profile function $g(r)$ is *almost* 1 everywhere.[10] These properties can be seen in Fig. 1.

From the solutions in Fig. 1 we determine the integration constants q_χ and q_G in the asymptotic solutions in Eqs. (4.9) and (4.10) as summarized in Table I.

Let us next focus on the color magnetic flux by looking at $h(r)$. The function $h(r)$ behaves almost similar among the cases of $\{m_G, m_\phi, m_\chi\} = \{1, 1, 1\}, \{1, 5, 1\}, \{1, 1, 5\}, \{1, 5, 5\}$ in Fig. 1 because of the common choice of $m_G = 1$. When the gluon mass is larger, $m_G = 5$, $h(r)$ becomes

[8]Remember that the exponential tails of the ANO vortices are like $e^{-m_H r}$ for the massive scalar field H with mass m_H and $e^{-m_e r}$ for the massive $U(1)$ gauge boson with mass m_e. The layer structures are exchanged for $m_e > m_H$ (type II) and $m_e < m_H$ (type I). Then their interactions depend on the ratio m_e/m_H giving classification of type I and II. However, for the strong type II region ($m_e > 2m_H$), the tail of the gauge field becomes $e^{-2m_H r}$ [27]. The width of the gauge field cannot become smaller than the half of that $1/m_H$ of the scalar field.

[9]A similar phenomenon is known for usual superconductors as denoted in footnote [8]. However the threshold is $m_e = 2m_H$ in that case.

[10]The approximation $g = 1$ used in Ref. [6] may be justified in the region $m_\phi \sim m_\chi$. However, since the relation $\lambda_1 = \lambda_2$ holds at weak coupling regime [6] the masses are related by $m_\phi = 2m_\chi$.

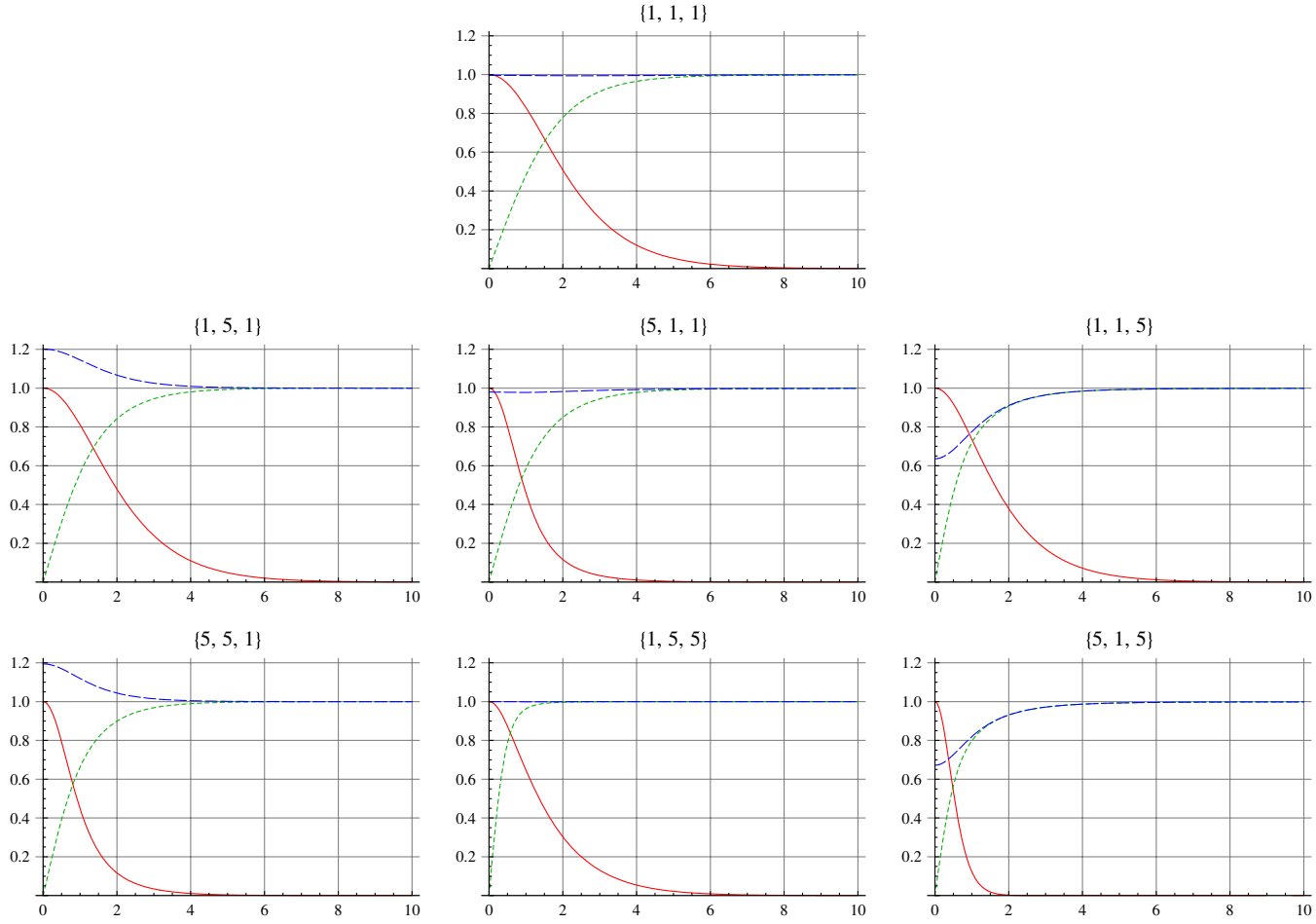

FIG. 1 (color online). The numerical solutions for several $\{m_G, m_\phi, m_\chi\}$. $[h(r), f(r), g(r)] =$ [R (solid line), G (short dashed line), B (long dashed line)]..

more sharp as can be seen in the cases of $\{5, 1, 1\}$ and $\{5, 5, 1\}$ in Fig. 1. The flux becomes far more sharp when we take $m_\chi \sim m_G$ as can be seen in the case of $\{5, 1, 5\}$ in Fig. 1. Qualitatively these behaviors match the result from the asymptotic tails in the previous section. In order to get a more quantitative width, let us define a width of the color magnetic flux by[11]

$$\langle r \rangle \equiv \sqrt{\frac{\int dx^2 F_{12}^8 r^2}{\int dx^2 F_{12}^8}} = \sqrt{\int_0^\infty dr r^2 h'}. \tag{5.1}$$

The numerical values of this quantity are shown in Fig. 2 for various values of m_G and m_χ. The left-upper panel of Fig. 2 shows that the width rapidly decreases for relatively small $m_G (\lesssim 4)$ and then approaches to a constant value for larger $m_G (\gtrsim 4)$. Contrary to this the Compton wavelength m_G^{-1} of the massive gluon goes down to zero as m_G increases. These behaviors are significantly different. Furthermore, the width approaches to a smaller constant at large m_G for larger m_χ as can be seen in the upper-right panel of Fig. 2. We thus find that the size of the color magnetic flux cannot become smaller than some value determined by the mass m_χ of the traceless scalar fields for the larger gluon mass m_G. This is consistent with the asymptotic behavior found in Eq. (4.9).

On the other hand, the size of the color magnetic flux is well approximated by the Compton wavelength m_G^{-1} when m_G changes with keeping $m_\chi = m_G$ as shown in the lower panel in Fig. 2. The result in this parameter region is complement to the last section, where it was difficult to study analytically.

VI. CONCLUSION AND DISCUSSION

In this paper we have studied the topologically stable vortex in the color superconductor. By using the relaxation method with the appropriate boundary conditions, we have presented numerical solutions for diverse choices of the

[11]The definition of this width has been given first in the study of a local $U(N)$ vortex [26] for which the phase $U(1)_B$ is gauged.

TABLE I. Several numerical values of q_χ and q_G. The case of $m_G = 2, 3, 4, 5 > m_\chi = 1$ [in Eq. (4.9)] and the case of $m_\chi = 2, 3, 4, 5 > m_G = 1$ [in Eq. (4.10)] are written in the upper and lower boxes, respectively. The parentheses beside q_χ and q_G imply that we evaluate these values by using the asymptotic tails δG or δh in Eq. (4.9) or Eq. (4.10). For q_χ we find a good agreement between $q_\chi(\delta G)$ and $q_\chi(\delta h)$. However for q_G it is not so good for smaller m_χ.

$m_G(m_\chi = m_\phi = 1)$	2	3	4	5
$q_\chi(\delta G)$	1.9(±0.1)	1.60(±0.03)	1.46(±0.03)	1.38(±0.02)
$q_\chi(\delta h)$	2.0(±0.1)	1.62(±0.01)	1.47(±0.02)	1.38(±0.01)
$m_\chi(m_G = m_\phi = 1)$	2	3	4	5
$q_G(\delta G)$	1.9(±0.1)	1.65(±0.1)	1.56(±0.05)	1.54(±0.05)
$q_G(\delta h)$	1.68(±0.03)	1.53(±0.02)	1.48(±0.02)	1.47(±0.02)

coupling constants (Fig. 1). We have found the asymptotic tails of the profile functions in Eqs. (4.9) and (4.10) and have determined their coefficients q_χ and q_G in Table I. Furthermore we have proposed the width $\langle r \rangle$ of the color flux tube as in Eq. (5.1) and have calculated it numerically. Contrary to the naive expectation, the width of the color

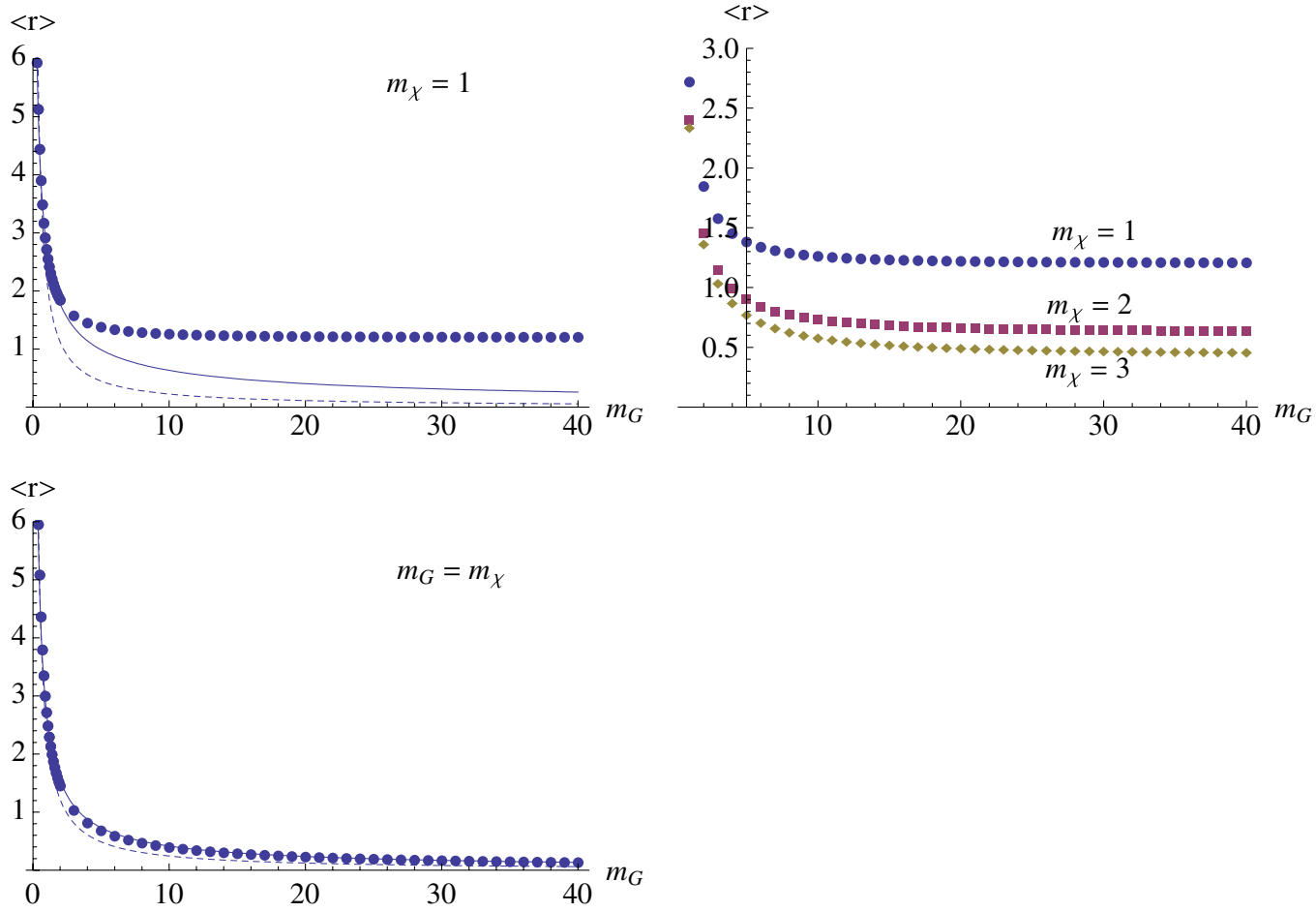

FIG. 2 (color online). The width $\langle r \rangle$ of the color flux tube in Eq. (5.1) vs the Compton wavelength m_G^{-1}. In the upper-left panel we plot the width $\langle r \rangle$ as dots in the cases of $m_\chi = 1$ and various m_G (with $m_\phi = 1$). The Compton wavelength $2.2/m_G$ is drawn by the broken curve in which the coefficient is determined by trying to fit it to the numerical points. (However they fit well nowhere.) The unbroken curve is $2.78 \times m_G^{-0.64}$ made by MATHEMATICA which fits very well at $m_G < 1$. In the upper-right panel the width $\langle r \rangle$ in the cases $m_\chi = 1, 2, 3$ (disk, box, diamond) are plotted (with $m_\phi = 1$). In the lower panel we plot the width $\langle r \rangle$ in the cases of $m_G = m_\chi$ (with $m_\phi = 1$). The broken curve denotes the Compton wavelength $2.4/m_G$ which fits to the data better than the case of upper-left panel. The unbroken curve denotes $2.72 \times m_G^{-0.82}$ which fits well to the data everywhere.

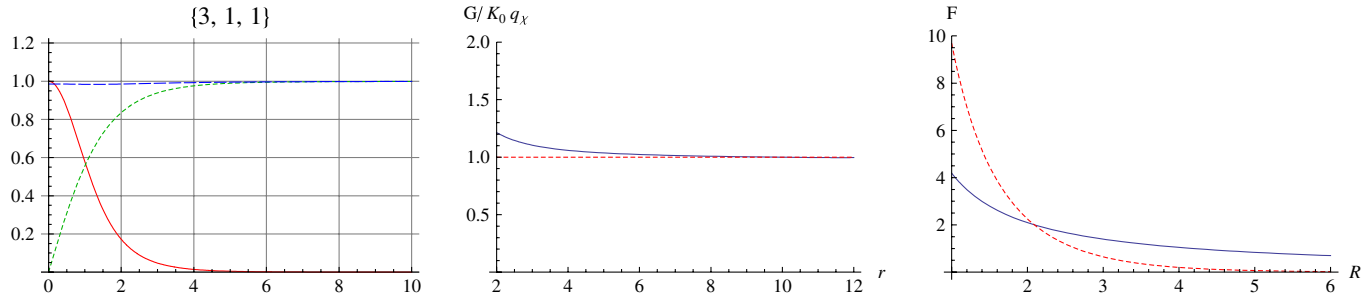

FIG. 3 (color online). The profile functions for $(m_\chi, m_\phi, m_G) = (1, 1, 3)$ in the leftmost panel $[h(r), f(r), g(r)] =$ [R (solid line), G (short dashed line), B (long dashed line)]. The middle panel shows the ratio $g/(q_\chi K_0(m_\chi r)) \sim 1$. A rough estimation of the long range and short range interactions are shown in the rightmost panel.

magnetic flux tube does not behave as the Compton wavelength (the penetration depth) m_G^{-1} of the massive gluons for the gluon mass m_G larger than the mass m_χ of the traceless scalar χ as shown in Fig. 2.

Here let us discuss the application of our result to the analysis of the interaction between two semisuperfluid vortices. As shown in [11], the long range interaction is mediated by the massless NG mode of the broken $U(1)_{\rm B}$. The universal repulsion between two vortices at distance $R(\gg m_{\phi,\chi,G}^{-1})$ was found [11] to be

$$F_{\rm long}(R) \simeq \frac{4\pi}{N_{\rm C} R}, \qquad N_{\rm C} = 3. \tag{6.1}$$

This force comes from the overlapping of the long power tails of the two vortices. When the vortices are placed at a relatively short distance $R \gtrsim m_{\phi,\chi,G}^{-1}$, we may find the exponential tails $e^{-m_\phi r}$, $e^{-m_\chi r}$, $e^{-m_G r}$. The overlapping of these tails yields the intervortex potential. For instance, when the tail of χ is overlapped for $m_\chi < m_G$, it can be written as

$$V_\chi(R) = C_\chi 2\pi q_\chi^2 K_0(m_\chi R). \tag{6.2}$$

Here R is the relative distance and q_χ is the parameter in Eq. (4.9). The function C_χ is unknown and should depend on the relative orientation of the two vortices in the internal space.[12] Thus the corresponding intervortex force is given by

$$F_\chi(R) = -\frac{\partial V_\chi}{\partial R} = C_\chi 2\pi q_\chi^2 m_\chi K_1(m_\chi R). \tag{6.3}$$

Let us compare these forces $F_{\rm long}$ and F_χ by extrapolating them near the vortex core. In the following we assume $C_\chi = O(1)$ for simplicity. As an example we choose $(m_\chi, m_\phi, m_G) = (1, 1, 3)$, see Fig. 3. The width $\langle r \rangle$ can be read as $r = 1.58$ from Fig. 2. The approximation $G = q_\chi K_0(m_\chi r)$, initially obtained for the large distance, is still valid up to $r \gtrsim 2$ as can be seen in the middle panel of Fig. 3. Therefore we can safely use Eq. (6.3) in this region. As one can see in the right panel of Fig. 3, the two kinds of the intervortex forces $F_{\rm long}$ and F_χ extrapolated to the near region of the core are comparable around $R = 2$. We conclude that the intervortex force mediated by the exchange of the massive particles like the massive gluons becomes comparable with the intervortex force mediated by the exchange of the massless $U(1)_{\rm B}$ NG boson. More precise discussion remains as a future problem. The detailed study of it is necessary to understand the lattice structure of non-Abelian semisuperfluid vortices when the lattice spacing is of the order of the penetration depth or the coherence length.

If the short range force is attractive, the vortex lattice collapses for high vortex density. There may appear composite vortices. The internal structure of a composite vortex may be ample which was studied in the case of local $U(N)$ vortices [29]. Other interesting aspects are dynamical collision (for instance the reconnection) of non-Abelian vortex strings [30] and a gas of non-Abelian vortices at finite temperature [31] (lower than transition temperature to quark gluon plasma phase), both of which were also studied in the case of local $U(N)$ vortices.

Let us make brief comments on possible application to the neutron star physics. In a response to the rapid rotation of a neutron star, superfluid vortices are created along the rotating axis in the outer core (the hadronic phase) where neutrons exhibit superfluidity. It was pointed out in the seminal paper by Anderson and Itoh [32] that those vortices may explain the pulsar glitch phenomenon. If the CFL phase is realized in the core of a neutron star, those superfluid vortices are somehow connected to $U(1)_{\rm B}$ superfluid vortices in the CFL phase. Each $U(1)_{\rm B}$ superfluid vortex must be divided into three semisuperfluid vortices (color flux tubes). Therefore color flux tubes are necessary ingredients in the study of neutron stars if the CFL phase is realized in the core. On the other hand, pulsars are accompanied with the large amount of magnetic fields of $U(1)_{\rm EM}$. Protons exhibit superconductivity in the hadronic phase, and so there should exist magnetic flux tubes along the axis

[12]For usual superconductors, $C_\chi = -1$ and this gives the attractive force.

of the magnetic fields. If those magnetic fields penetrate into the CFL phase realized in the core, there is no topological reason for those fluxes to be squeezed, because the $U(1)_{\rm EM}$ symmetry (with mixed with one color component) is not broken there. It was, however, pointed out that fluxes are squeezed into flux tubes there [13] where the CFL phase is modified by large magnetic fields [33]. In general, the axes of the rotation and the magnetic fields of the pulsar are different with some angle, the interaction between the (electro)magnetic fluxes and the color magnetic fluxes studied in this paper should be important in the study of the neutron stars.

ACKNOWLEDGMENTS

We would like to thank Eiji Nakano for discussions in the early stages of this paper and Naoki Yamamoto for useful comments. The work of M. E. is supported by Special Postdoctoral Researchers Program at RIKEN. The work of M. N. is supported in part by Grant-in-Aid for Scientific Research (No. 20740141) from the Ministry of Education, Culture, Sports, Science and Technology-Japan.

APPENDIX: GENERAL DIAGONAL SOLUTIONS

In this Appendix we study more general diagonal vortex solutions. They can be obtained as follows:

$$\Phi(r,\theta) = e^{i\theta((1/\sqrt{3})T_0 - \sqrt{(2/3)}(\nu_3 T_3 + \nu_8 T_8))} \times \left(\frac{F(r)}{\sqrt{3}} T_0 - \frac{\sqrt{2}G(r)}{\sqrt{3}}(\nu_3 T_3 + \nu_8 T_8)\right), \quad \text{(A1)}$$

$$A_i(r,\theta) = \frac{1}{g_s}\frac{\epsilon_{ij}x^j}{r^2}[1 - h(r)]\sqrt{\frac{2}{3}}(\nu_3 T_3 + \nu_8 T_8), \quad \text{(A2)}$$

where we have defined the Cartan subalgebra $\{T_0, T_3, T_8\}$ of $U(3)$ by

$$T_0 = \frac{1}{\sqrt{3}}\mathrm{diag}(1,1,1), \qquad T_3 = \frac{1}{\sqrt{2}}\mathrm{diag}(0,1,-1), \qquad T_8 = \frac{1}{\sqrt{6}}\mathrm{diag}(-2,1,1). \quad \text{(A3)}$$

The parameters ν_3 and ν_8 are determined by the requirement of the single valuedness of the fields, $e^{i2\pi((1/\sqrt{3})T_0 - \sqrt{(2/3)}(\nu_3 T_3 + \nu_8 T_8))} = 1$. Three solutions are found: $(\nu_3, \nu_8) = (0,1), (\pm\sqrt{3}/2, -1/2)$. For instance, in the case of $(\nu_3, \nu_8) = (0,1)$ we find the solutions for Eq. (3.1) with

$$f = \frac{F + 2G}{3}, \qquad g = \frac{F - G}{3}. \quad \text{(A4)}$$

This solution with $(\nu_3, \nu_8) = (\pm\sqrt{3}/2, -1/2)$ constitutes the weight vectors of **3**.

[1] M. G. Alford, K. Rajagopal, and F. Wilczek, Phys. Lett. B **422**, 247 (1998); Nucl. Phys. **B537**, 443 (1999).
[2] M. G. Alford, Annu. Rev. Nucl. Part. Sci. **51**, 131 (2001); M. G. Alford, A. Schmitt, K. Rajagopal, and T. Schafer, Rev. Mod. Phys. **80**, 1455 (2008).
[3] A. A. Abrikosov, Zh. Eksp. Teor. Fiz. **32**, 1442 (1957) [Sov. Phys. JETP **5**, 1174 (1957)].
[4] H. B. Nielsen and P. Olesen, Nucl. Phys. **B61**, 45 (1973).
[5] I. Giannakis and H. c. Ren, Nucl. Phys. **B669**, 462 (2003).
[6] A. P. Balachandran, S. Digal, and T. Matsuura, Phys. Rev. D **73**, 074009 (2006).
[7] I. Giannakis and H. c. Ren, Phys. Rev. D **65**, 054017 (2002).
[8] K. Iida and G. Baym, Phys. Rev. D **66**, 014015 (2002).
[9] K. Iida, Phys. Rev. D **71**, 054011 (2005).
[10] M. M. Forbes and A. R. Zhitnitsky, Phys. Rev. D **65**, 085009 (2002).
[11] E. Nakano, M. Nitta, and T. Matsuura, Phys. Rev. D **78**, 045002 (2008).
[12] E. Nakano, M. Nitta, and T. Matsuura, Prog. Theor. Phys. Suppl. **174**, 254 (2008).
[13] E. J. Ferrer and V. de la Incera, Phys. Rev. Lett. **97**, 122301 (2006); J. Phys. A **40**, 6913 (2007).
[14] J. Liao and E. Shuryak, Phys. Rev. C **75**, 054907 (2007); M. N. Chernodub and V. I. Zakharov, Phys. Rev. Lett. **98**, 082002 (2007); M. N. Chernodub, A. Nakamura, and V. I. Zakharov, Phys. Rev. D **78**, 074021 (2008).
[15] J. Liao and E. Shuryak, Phys. Rev. C **77**, 064905 (2008).
[16] A. Hanany and D. Tong, J. High Energy Phys. 07 (2003) 037; R. Auzzi, S. Bolognesi, J. Evslin, K. Konishi, and A. Yung, Nucl. Phys. **B673**, 187 (2003); M. Eto, Y. Isozumi, M. Nitta, K. Ohashi, and N. Sakai, Phys. Rev. Lett. **96**, 161601 (2006).
[17] D. Tong, arXiv:hep-th/0509216; M. Eto, Y. Isozumi, M. Nitta, K. Ohashi, and N. Sakai, J. Phys. A **39**, R315 (2006); M. Shifman and A. Yung, Rev. Mod. Phys. **79**, 1139 (2007); D. Tong, Ann. Phys. (N.Y.) **324**, 30 (2009).
[18] M. Eto, E. Nakano, and M. Nitta, arXiv:0908.4470 [Phys. Rev. D (to be published)].

[19] D. M. Sedrakian, D. Blaschke, K. M. Shahabasyan, and M. K. Shahabasyan, Astrophysics (Engl. Transl.) **51**, 544 (2008).
[20] K. Iida and G. Baym, Phys. Rev. D **63**, 074018 (2001); **66**, 059903(E) (2002).
[21] K. Iida and G. Baym, Phys. Rev. D **65**, 014022 (2001).
[22] A. P. Balachandran and S. Digal, Phys. Rev. D **66**, 034018 (2002); Int. J. Mod. Phys. A **17**, 1149 (2002).
[23] M. Nitta and N. Shiiki, Phys. Lett. B **658**, 143 (2008).
[24] E. Nakano, M. Nitta, and T. Matsuura, Phys. Lett. B **672**, 61 (2009).
[25] M. Eto, E. Nakano, and M. Nitta, Nucl. Phys. **B821**, 129 (2009).
[26] M. Eto, T. Fujimori, T. Nagashima, M. Nitta, K. Ohashi, and N. Sakai, Phys. Lett. B **678**, 254 (2009).
[27] B. Plohr, J. Math. Phys. (N.Y.) **22**, 2184 (1981); L. Perivolaropoulos, Phys. Rev. D **48**, 5961 (1993).
[28] R. Auzzi, M. Eto, and W. Vinci, J. High Energy Phys. 11 (2007) 090; 02 (2008) 100.
[29] M. Eto, K. Konishi, G. Marmorini, M. Nitta, K. Ohashi, W. Vinci, and N. Yokoi, Phys. Rev. D **74**, 065021 (2006).
[30] M. Eto, K. Hashimoto, G. Marmorini, M. Nitta, K. Ohashi, and W. Vinci, Phys. Rev. Lett. **98**, 091602 (2007).
[31] M. Eto, T. Fujimori, M. Nitta, K. Ohashi, K. Ohta, and N. Sakai, Nucl. Phys. **B788**, 120 (2008).
[32] P. W. Anderson and N. Itoh, Nature (London) **256**, 25 (1975).
[33] E. J. Ferrer, V. de la Incera, and C. Manuel, Phys. Rev. Lett. **95**, 152002 (2005); Nucl. Phys. **B747**, 88 (2006); E. J. Ferrer and V. de la Incera, Phys. Rev. D **76**, 045011 (2007); **76**, 114012 (2007).